

Direct evidence of uneven d_{xz} and d_{yz} orbital occupation in the superconducting state of iron pnictideDamian Rybicki^{1,*}, Marcin Sikora^{2,†}, Joanna Stępień², Łukasz Gondek¹, Kamil Goc¹, Tomasz Strączek¹, Michał Jurczyszyn², Czesław Kapusta¹, Zbigniew Bukowski³, Michał Babij³, Marcin Matusiak^{3,4} and Marcin Zajac⁵¹AGH University of Science and Technology, Faculty of Physics and Applied Computer Science,

Department of Solid State Physics, al. A. Mickiewicza 30, 30-059 Kraków, Poland

²AGH University of Science and Technology, Academic Centre for Materials and Nanotechnology,

al. A. Mickiewicza 30, 30-059 Kraków, Poland

³Institute of Low Temperature and Structure Research, Polish Academy of Sciences, Okólna 2, 50-422 Wrocław, Poland⁴International Research Centre MagTop, Institute of Physics, Polish Academy of Sciences, Aleja Lotników 32/46, PL-02668 Warszawa, Poland⁵National Synchrotron Radiation Centre SOLARIS, Jagiellonian University, Czerwone Maki 98, 30-392 Kraków, Poland

(Received 24 June 2020; revised 29 October 2020; accepted 29 October 2020; published 16 November 2020)

The origin of nematicity and its relation to superconductivity in iron pnictide high-temperature superconductors remains unclear. One of its possible sources is the uneven occupation of Fe d_{xz} and d_{yz} orbitals. Here, by using x-ray linear dichroism technique, we show that such an imbalance is present in $\text{Eu}(\text{Fe}_{1-x}\text{Co}_x)_2\text{As}_2$ single crystals deep in the tetragonal phase and also in the superconducting state, where we find that the d_{xz} orbital has a higher occupation as indicated by an x-ray linear dichroism magnitude of 1.5%. Our result shows the importance of orbital polarization in the theoretical description of nematicity and superconductivity, particularly for determination of the superconducting gap symmetry, which is affected by orbital fluctuations.

DOI: [10.1103/PhysRevB.102.195126](https://doi.org/10.1103/PhysRevB.102.195126)**I. INTRODUCTION**

The presence of different types of order and phase transitions can be regarded as a characteristic of high-temperature superconductors. In the cuprates, except for the superconductivity, one has to consider antiferromagnetic order, pseudogap, and charge density fluctuations. In iron pnictides, one has to typically add spin-density wave and structural phase transition. These two are connected to nematicity, which was first observed in underdoped compounds from anisotropy of the in-plane resistivity that was also present above the structural/magnetic phase transition [1]. Up to now, nematic fluctuations have been observed by several techniques, also in optimally doped and overdoped materials or families with no structural/magnetic phase transition [2–10]. Moreover, recent studies demonstrated that nematicity shows strong spatial variation [11–14], which makes the description of these materials even more complex. Of particular interest, with regard to nematicity and superconductivity, is the importance of the orbital degrees of freedom [15], with the key role played by Fe d_{xz} and d_{yz} orbitals. The unexpected difference in occupation of those orbitals, also in the tetragonal phase, was first reported from scanning tunneling microscope (STM) [16] and angle-resolved photoemission spectroscopy (ARPES) [17] studies, and indicated that nematicity is rather of electronic than structural origin. Here, by using x-ray absorption spectroscopy and x-ray linear dichroism, which allows us to measure the difference of occupation of said Fe

orbitals in the superconducting state, we show that such a difference is present well above structural phase transition, but more importantly, also below the critical temperature of superconductivity, T_c in $\text{Eu}(\text{Fe}_{1-x}\text{Co}_x)_2\text{As}_2$ single crystals.

II. EXPERIMENTAL

Preparation and characterization of $\text{Eu}(\text{Fe}_{1-x}\text{Co}_x)_2\text{As}_2$ single crystals is thoroughly described in literature [18]. We studied two single crystals, undoped EuFe_2As_2 exhibiting simultaneous spin density wave and tetragonal/orthorhombic structural transition at $T_{\text{SDW}}=T_s \approx 190$ K, and the temperature of Eu magnetic ordering (T_{Eu}) equal to 19 K. The second crystal was an electron doped (underdoped) superconductor $\text{EuFe}_{1.8}\text{Co}_{0.2}\text{As}_2$ (i.e., with $x=0.1$) of T_{SDW} and $T_s \approx 130$ K–135 K, $T_{\text{Eu}}=17$ K, and $T_c=10$ K.

An x-ray diffraction (XRD) study was done on powdered samples at Panalytical Empyrean powder diffractometer in the Bragg-Brentano geometry. An x-ray tube with Cu anode was used for measurements. For low-temperature XRD studies, an Oxford Instruments PheniX closed-cycle helium refrigerator was used (14 K–300 K). During the low-temperature measurements, the sample position was corrected against thermal displacement of the sample stage. Temperature stabilization was better than 0.1 K. The XRD patterns were refined using the Rietveld-type package FULLPROF [19].

X-ray absorption spectroscopy (XAS) measurements were performed at the PEEM/XAS beamline of Solaris National Synchrotron Radiation Centre, Poland [20]. The spectra were collected at the $L_{3,2}$ edge of Fe using total electron yield detection mode. Before collecting XAS spectra, the crystals were cleaved *in situ* (under vacuum better than 7.5×10^{-7} mbar).

*ryba@agh.edu.pl

†marcins@agh.edu.pl

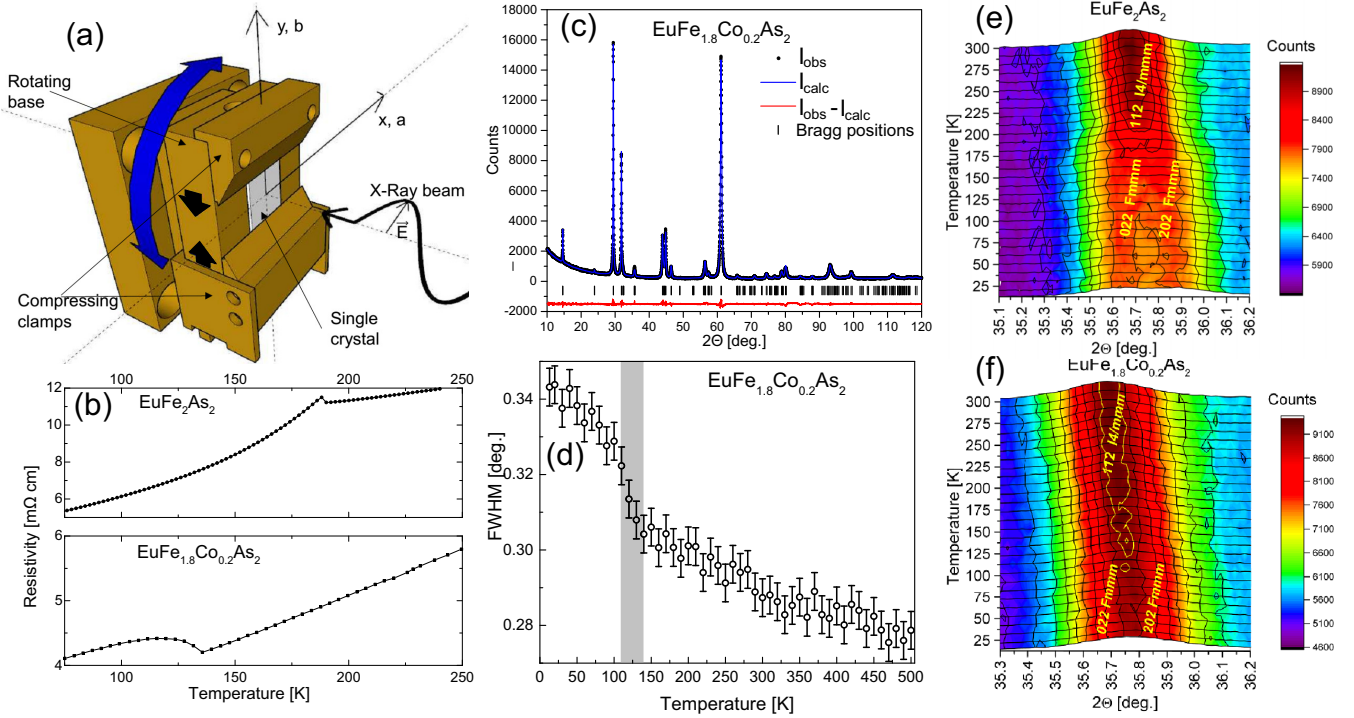


FIG. 1. (a) A scheme of the experimental setup showing the device for mechanical detwinning of single crystals and geometry of XAS experiments. The arrows show the direction of pressing and rotation; a and b (with $a > b$) indicate lattice parameters in the orthorhombic phase with respect to the polarization E of the incoming x-ray radiation. (b) Temperature dependence of electrical resistivity close to the structural phase transition. (c) Diffraction pattern and (d) full width at half maximum (FWHM) of the reflection at 35.75° of Co doped sample. (e), (f) Temperature dependence of characteristic reflections: 022, 202 of $Fm\bar{m}m$ space group and 112 of $I4/m\bar{m}m$ space group.

For mechanical detwinning of single crystals by applying uniaxial pressure, we used a specially designed sample holder. It allowed for 90 degrees rotation inside the experimental chamber to change the angle between crystal axes and light polarization direction for detecting the x-ray linear dichroism signal (XLD). The experimental setup and geometry are schematically shown in Fig. 1(a). Prior to XAS measurements single crystals were cut at a 45-degree angle with respect to the tetragonal a axis.

III. RESULTS AND DISCUSSION

To carry out analysis of the XLD signal, particularly to evaluate the structural contribution as described by Kim *et al.* [21], we conducted detailed XRD studies. XRD patterns of both $\text{Eu}(\text{Fe}_{1-x}\text{Co}_x)_2\text{As}_2$ samples at 300 K can be indexed by the tetragonal $I4/m\bar{m}m$ space group (No. 139). An example of the collected full-range diffraction patterns is presented in Fig. 1(c). Low temperature XRD studies revealed that for the undoped sample, a structural transition takes place at about 190 K, as shown in Fig. 1(e). The low-temperature structure of the pristine EuFe_2As_2 shows the orthorhombic ($Fm\bar{m}m$ space group) symmetry. The most prominent change can be noticed around 35.75° of 2θ , where the 112 reflection of the high-temperature tetragonal phase ($I4/m\bar{m}m$) splits into two 022 and 202 reflections of the low-temperature one ($Fm\bar{m}m$). In contrast to that, for $\text{EuFe}_{1.8}\text{Co}_{0.2}\text{As}_2$ the evolution of the 112 reflection is not so pronounced and no splitting is visible, suggesting that this transition is far less defined than for the

undoped sample. The presence of the structural transition can only be deduced from the temperature dependence of the width of this reflection and the related intensity change as shown in Fig. 1(d). The full width at half maximum that increases gradually with decreasing temperature shows a pronounced step in the temperature range 110–140 K.

Resistivity measurements show that, in the case of the undoped compound, there is a sharp upturn at the phase transition temperature and this upturn shifts to lower temperatures and broadens with Co doping (Fig. 1(b) and Ref. [18]), which is consistent with our XRD measurements. The Fermi surface of the iron-pnictides undergoes a reconstruction at the magnetostructural transition [22]. This leads to the formation of Dirac cones [23], which can significantly participate in the electronic transport due to high mobility of Dirac fermions [24]. As a result, the resistivity of the EuFe_2As_2 parent compound decreases in the spin-density-wave state, as can be seen in the top panel of Fig. 1(b). On the other hand, the contribution from Dirac fermions was shown to vanish quickly with cobalt doping [25]. In the absence of highly mobile charge carriers, the resistivity in the magnetic phase of the electron-doped 122-pnictides increases, interestingly, mostly along the b axis [9]. In twinned crystals, this leads to an increase of the overall resistivity, which is the average of a - and b - axes values [see the bottom panel of Fig. 1(b)]. Such behavior can, for example, be caused by strongly anisotropic scattering of charge carriers [26] or large variations of the Drude weight [27].

Recent x-ray and neutron scattering results on other compounds from the 122 family, namely, $(\text{Sr}, \text{Na})\text{Fe}_2\text{As}_2$, revealed

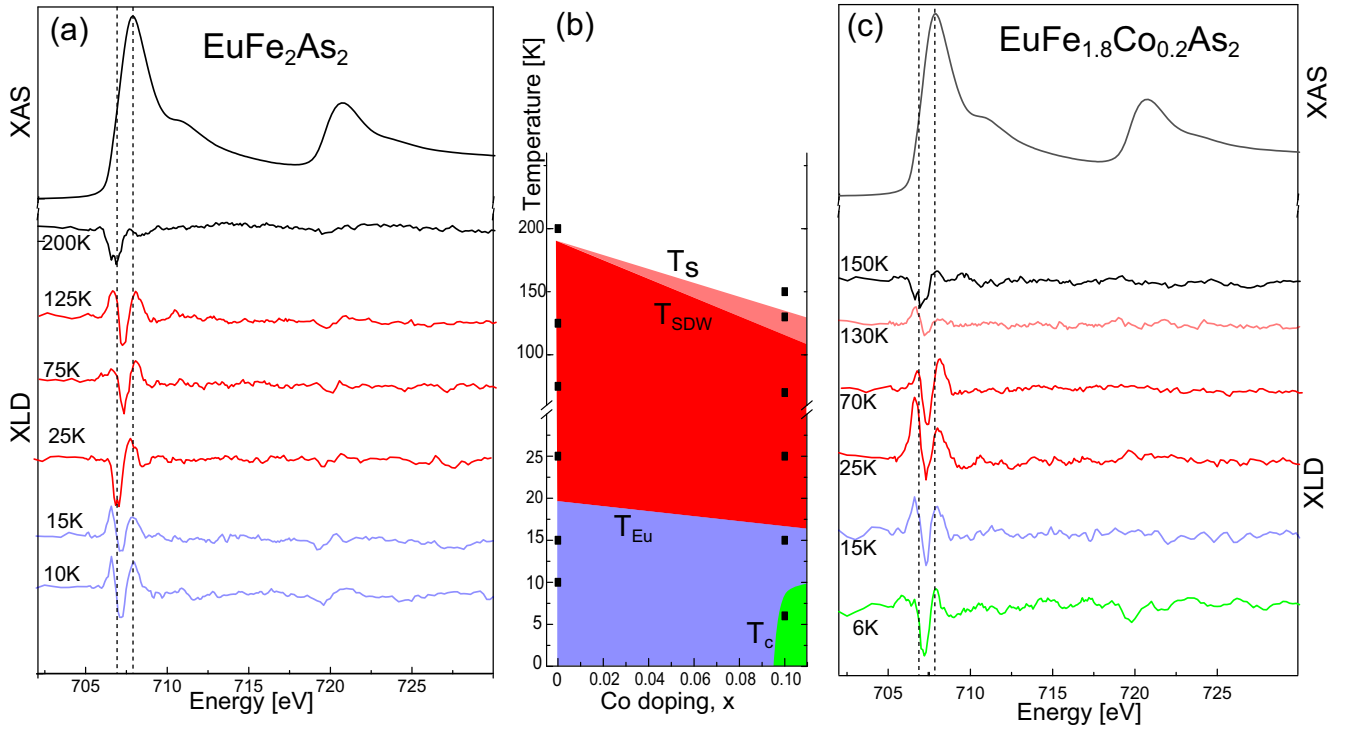


FIG. 2. Fe $L_{3,2}$ edge XAS spectrum for (a) undoped EuFe_2As_2 and (c) Co doped $\text{EuFe}_{1.8}\text{Co}_{0.2}\text{As}_2$ ($x = 0.1$) measured at 150 K and XLD spectra at selected temperatures for both samples. Panel (b) schematically shows the phase diagram [18], solid points indicate temperatures for which XLD results are shown in (a) and (c) panels.

the presence of short length scale (1–3 nm) orthorhombic distortions of the instantaneous local structure in compounds with overall tetragonal symmetry. These local structural fluctuations are present at temperatures much higher than T_s and occur even in highly doped compounds, which do not show structural phase transitions [12,13]. Also, other results, e.g., from elastic measurements or ARPES, indicate the presence of spatially varying structural and electronic fluctuations even in optimally doped and overdoped samples [2,14].

We now proceed to our main results, i.e., XAS and XLD. Figure 2 presents an example of the Fe $L_{3,2}$ edge XAS spectra for both single crystals studied, which look typical for iron pnictides and metallic materials with Fe in the high-spin state and with weak electronic correlations [28–30]. There are two white lines in the spectra, which result from $2p$ to $3d$ dipole transitions ($2p^6 3d^6 \rightarrow 2p^5 3d^7$) with spin-orbit split $2p$ states $2p_{3/2}$ (L_3) and $2p_{1/2}$ (L_2), which are located at about 708 eV and 721 eV, respectively. No distinct multiplet features are visible.

As in previous studies on compounds from the 122 family, we found that for a given orientation, the Fe $L_{3,2}$ XAS spectra do not show noticeable temperature or doping dependence [21,31–33]. However, if we take a difference between normalized spectra measured for different orientations of the x-ray polarization vector E and crystal axes, we obtain a clear XLD signal for both single crystals (Fig. 2). To calculate the XLD signal, we take $I_x - I_y$, with x and y as defined in Fig. 1(a), i.e., I_x is the intensity of the XAS spectrum measured for E parallel to the a lattice parameter (I_y , $E \parallel b$). Our XLD spectra are similar in shape to those obtained for $\text{Ba}(\text{Fe}_{1-x}\text{Co}_x)_2\text{As}_2$ [21] and we also observe the XLD signal at temperatures

significantly higher than T_s . In principle, in the tetragonal phase there should be no difference between the I_x and I_y XAS spectra. However, several experimental techniques in various iron pnictide materials reported anisotropic in-plane properties to also be present above T_s , which are generally referred to as nematic fluctuations, in contrast to nematic order present below T_s . These fluctuations can be of structural/spin/orbital origin and have also been observed in the Eu-based 122 family according to the resistivity and thermopower measurements [34,35].

The origin of an XLD signal in iron pnictides can be twofold [36]. First, there may be a contribution coming from the structural anisotropy. While in the high-temperature tetragonal phase, the crystals have the overall C_4 symmetry and no in-plane anisotropy can be expected, below T_s in the orthorhombic phase, the C_4 symmetry is broken and one expects a contribution from structural anisotropy due to a small difference between a and b lattice parameters (less than 1%). Second, there could be a contribution due to unequal occupation of orbitals that are probed in measurement along a and b directions. In the case of the Fe $L_{3,2}$ edge in iron pnictides, those orbitals are d_{xz} and d_{yz} , respectively [36].

The shape of both structural and orbital contributions has been theoretically calculated and the total XLD was predicted to reach up to a few percent relative to the total XAS signal [36]. This is what was found for $\text{Ba}(\text{Fe}_{1-x}\text{Co}_x)_2\text{As}_2$ [21] and in the present study for $\text{Eu}(\text{Fe}_{1-x}\text{Co}_x)_2\text{As}_2$. Those contributions, depending on the incident photon energy, can be positive or negative and might even cancel out. Therefore, a careful separation is needed to obtain their temperature and doping dependence. Such a refinement procedure has been

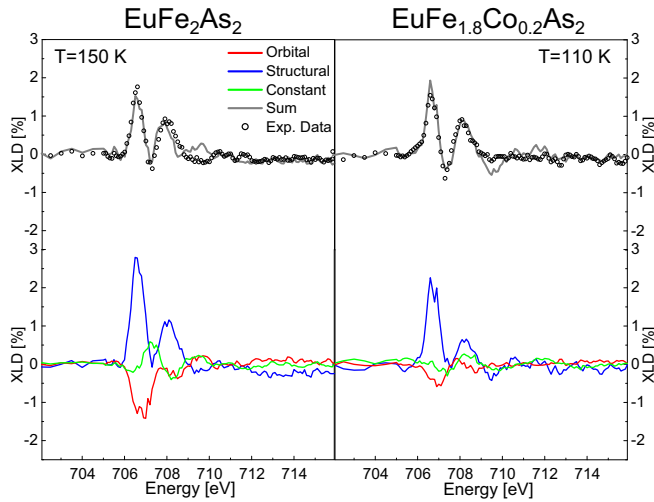


FIG. 3. Total experimental XLD signal (open black circles), the calculated structural (blue line), orbital (red line), constant (green line) contributions, and their sum (gray line) at selected temperatures for undoped EuFe_2As_2 (left panel) and $\text{EuFe}_{1.8}\text{Co}_{0.2}\text{As}_2$ (right panel).

formulated by Kim *et al.* [21] and we follow it, describing only the most important steps (more information in the Supplemental Material) [37–41]. As in Ref. [21], we observe an XLD signal at the highest temperatures, which possibly results from a small sample misalignment and a corresponding admixture of the out-of-plane (i.e., for $E \parallel c$) component related to the anisotropy between the c axis and aa (or ab) plane. We stress that for both single crystals, this contribution is significantly smaller compared to orbital and structural ones (Fig. 3).

Similar to $\text{Ba}(\text{Fe}_{1-x}\text{Co}_x)_2\text{As}_2$ [21], we observe that around T_s (190 K for undoped and 135 K for Co doped sample), the shape of the total XLD signal drastically changes and even changes its sign (Fig. 2). This behavior of the XLD signal is an indication of the structural phase transition and the appearance of the finite (assumed to be constant) structural contribution [21]. The assumption of constant structural component is supported by the fact that the relative change of the ratio of lattice parameters (a/b) in the orthorhombic phase is of the order of 0.1% or less [37]. Following Kim *et al.*, we calculated the structural and orbital contributions, which are presented in Fig. 3. We would also like to note that both contributions are of opposite signs and, thus, partly cancel each other at low temperatures, as was observed for $\text{Ba}(\text{Fe}_{1-x}\text{Co}_x)_2\text{As}_2$ [21] and predicted theoretically [36].

We now discuss the temperature dependence of the orbital contribution. First, one can notice that in both compounds, in the entire temperature range the orbital contribution is negative. Since it is due to the difference in occupation of d_{xz} and d_{yz} orbitals, one concludes that there are more empty states in the d_{yz} orbital, i.e., it is less occupied. This is in agreement with previous XLD studies on $\text{Ba}(\text{Fe}_{1-x}\text{Co}_x)_2\text{As}_2$ [21] but also with ARPES results, which indicate that once the material transforms from the tetragonal to orthorhombic structure, previously degenerated d_{yz} and d_{xz} orbitals split, and d_{yz} shifts up whereas d_{xz} shifts down in energy [15,17,42]. The orbital contribution is present at temperatures roughly by

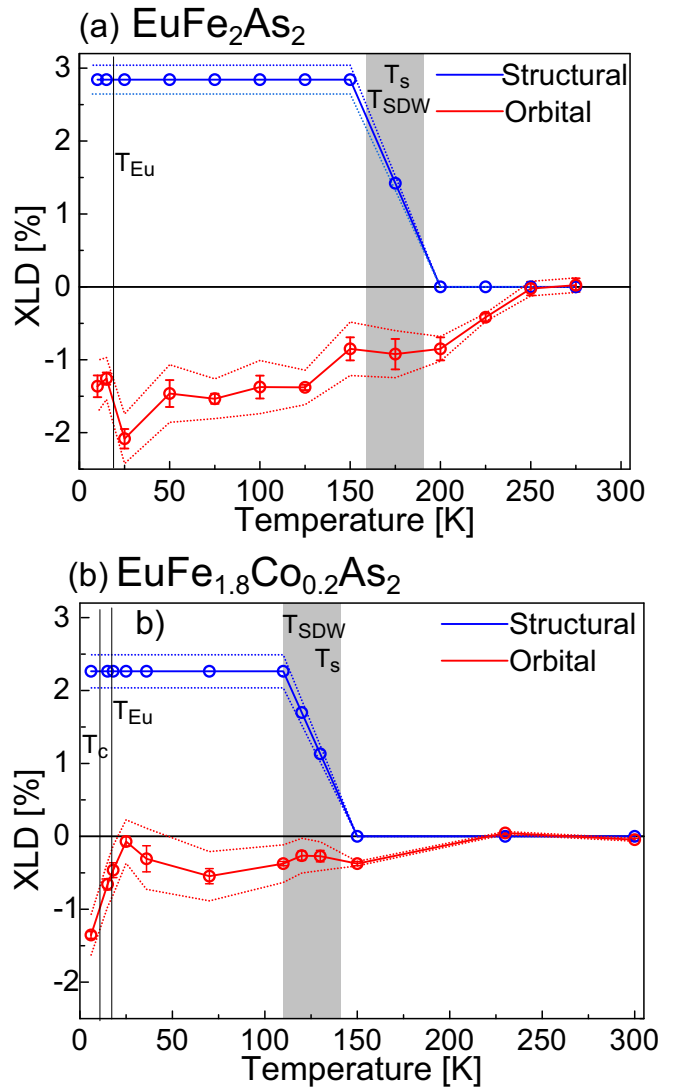


FIG. 4. Temperature dependence of the structural (blue) and orbital (red) contributions to the XLD signal for the undoped EuFe_2As_2 and $\text{EuFe}_{1.8}\text{Co}_{0.2}\text{As}_2$ single crystals. Dotted lines show the uncertainty margin. The shaded area corresponds to the temperature range of an abrupt change in the width (or splitting) of the reflection at 35.75° shown in Fig. 1(d) [Fig. 1(e)].

50 K higher than T_s , indicating unequal occupation of d_{yz} and d_{xz} orbitals deep in the tetragonal phase. The magnitude of the orbital contribution decreases with increasing temperature, as anticipated by the theory [36,43].

For the Co-doped crystal, the total XLD signal, the orbital contribution and its temperature dependence appear to be weaker compared to the undoped sample. While this could be expected, as the replacement of Fe by Co is an electron doping, we admit that it may also be a result of experimental precision limitations (crystal alignment, x-ray polarization) [21]. Therefore, quantitative comparison of bare values of structural and orbital contributions seems superfluous. We can, however, discuss more quantitatively the ratio of the orbital to structural component (O/S), which is not affected by experimental artifacts. As the relative difference between lattice parameters ($(a-b)/a$) is slightly bigger for the undoped

compound (1.0% vs 0.7%) one expects that the structural component should be proportionally larger for the undoped compound. This is indeed well reproduced in the experiment (see Fig. 4). In the temperature range between T_{Eu} and T_s , the ratio O/S amounts to approximately 0.5 and 0.2 for the undoped and Co doped material, respectively. One can then conclude that the relative value of the orbital component is significantly smaller in the Co-doped sample, which may be attributed mainly to reduced imbalance between d_{yz} and d_{xz} orbitals of Fe due to structural disorder caused by Co doping.

We observe that when the temperature decreases and approaches T_c , the magnitude of the orbital contribution starts to increase and remains nonzero in the superconducting state with XLD amplitude of 1.5% [Fig. 4(b)]. It is worth noting that our observation of an XLD signal in the superconducting state is, to our knowledge, unprecedented. A possible origin of this change of XLD signal close to T_c in magnetic ordering of Eu moments can be discarded as our XRD measurements do not show noticeable structural changes around T_{Eu} . Also, resistivity measurements on detwinned single crystals do not show a change of its anisotropy close to T_{Eu} either [34]. Mössbauer measurements indicate the appearance of a transferred contribution to the magnetic hyperfine field on Fe nuclei at T_{Eu} [44,45]. However, this is related to the polarization of the s -like conduction electrons and not to the modifications in the Fe $3d$ orbitals due to Eu ordering. These Fe orbitals are predominantly hybridized with As $4s/4p$ states [31] and a possible Eu influence could only be indirect and very weak.

On the other hand, it has recently been shown that the transition to the superconducting state can significantly affect the nematic order. Nematic correlation length, which peaks at T_c , strongly decreases in the superconducting state [46], which suggests that although nematic order can still be present below T_c [47,48], it actually competes with superconductivity [46].

Orbital fluctuations may play an important role in determining the symmetry of the superconducting gap in iron pnictides, although their significance depends on their relative strength compared to spin fluctuations, see, e.g., Ref. [49]. Theoretical calculations predict that orbital fluctuations would lead to the s_{++} type, while if the pairing is induced by antiferromagnetic spin fluctuations, it would lead to the s_{+-} type [50]. However, up to now there is no consensus regarding the gap symmetry in iron pnictides, for more information see Refs. [15,49,51]. With Co (electron) doping, not only the d_{xz}/d_{yz} hole pockets vanish, but also their energy splitting decreases as has been shown for $LiFe_{1-x}Co_xAs$ [4]. This is consistent with our findings.

Our results show convincingly the presence of the nematicity due to the structural anisotropy and the imbalance in the occupation of d_{yz} and d_{xz} orbitals of Fe. Unequal occupation of these orbitals already occurs in the high-temperature tetragonal phase but also persists in the superconducting state of the Eu-based 122 family. This points to the importance of interplay of orbital, structural, and also spin degrees of freedom in iron-based superconductors.

ACKNOWLEDGMENTS

This work was supported by the National Science Centre, Poland (Grant No. 2018/30/E/ST3/00377). Z.B. and M.B. acknowledge financial support from the National Science Centre, Poland (Grant No. 2017/25/B/ST3/02868). M.M. acknowledges support from the Foundation for Polish Science through the IRA Programme cofinanced by EU within SG OP and from the National Science Centre, Poland (Grant No. 2014/15/B/ST3/00357). Experiments were performed owing to the collaboration of SOLARIS Staff.

-
- [1] J.-H. Chu, J. G. Analytis, K. De Greve, P. L. McMahon, Z. Islam, Y. Yamamoto, and I. R. Fisher, *Science* **329**, 824 (2010).
 - [2] M. Yoshizawa, D. Kimura, T. Chiba, S. Simayi, Y. Nakanishi, K. Kihou, C.-H. Lee, A. Iyo, H. Eisaki, M. Nakajima, and S.-i. Uchida, *J. Phys. Soc. Jap.* **81**, 024604 (2012).
 - [3] A. E. Böhmer, P. Burger, F. Hardy, T. Wolf, P. Schweiss, R. Fromknecht, M. Reinecker, W. Schranz, and C. Meingast, *Phys. Rev. Lett.* **112**, 047001 (2014).
 - [4] H. Miao, L.-M. Wang, P. Richard, S.-F. Wu, J. Ma, T. Qian, L.-Y. Xing, X.-C. Wang, C.-Q. Jin, C.-P. Chou, Z. Wang, W. Ku, and H. Ding, *Phys. Rev. B* **89**, 220503(R) (2014).
 - [5] Z. Liu, Y. Gu, W. Zhang, D. Gong, W. Zhang, T. Xie, X. Lu, X. Ma, X. Zhang, R. Zhang, J. Zhu, C. Ren, L. Shan, X. Qiu, P. Dai, Y.-f. Yang, H. Luo, and S. Li, *Phys. Rev. Lett.* **117**, 157002 (2016).
 - [6] F. Kretzschmar, T. Böhm, U. Karahasanović, B. Muschler, A. Baum, D. Jost, J. Schmalian, S. Caprara, M. Grilli, C. Di Castro, J. G. Analytis, J.-H. Chu, I. R. Fisher, and R. Hackl, *Nature Phys.* **12**, 560 (2016).
 - [7] P. Massat, D. Farina, I. Paul, S. Karlsson, P. Strobel, P. Toulemonde, M.-A. Méasson, M. Cazayous, A. Sacuto, S. Kasahara, T. Shibauchi, Y. Matsuda, and Y. Gallais, *Proc. Natl. Acad. Sci.* **113**, 9177 (2016).
 - [8] W. Wang, Y. Song, C. Cao, K.-F. Tseng, T. Keller, Y. Li, L. W. Harriger, W. Tian, S. Chi, R. Yu, A. H. Nevidomskyy, and P. Dai, *Nat Commun* **9**, 3128 (2018).
 - [9] M. Matusiak, K. Rogacki, and T. Wolf, *Phys. Rev. B* **97**, 220501(R) (2018).
 - [10] X. Liu, R. Tao, M. Ren, W. Chen, Q. Yao, T. Wolf, Y. Yan, T. Zhang, and D. Feng, *Nat Commun* **10**, 1039 (2019).
 - [11] E. Thewalt, I. M. Hayes, J. P. Hinton, A. Little, S. Patankar, L. Wu, T. Helm, C. V. Stan, N. Tamura, J. G. Analytis, and J. Orenstein, *Phys. Rev. Lett.* **121**, 027001 (2018).
 - [12] B. A. Frandsen, K. M. Taddei, M. Yi, A. Frano, Z. Guguchia, R. Yu, Q. Si, D. E. Bugaris, R. Stadel, R. Osborn, S. Rosenkranz, O. Chmaissem, and R. J. Birgeneau, *Phys. Rev. Lett.* **119**, 187001 (2017).
 - [13] B. A. Frandsen, K. M. Taddei, D. E. Bugaris, R. Stadel, M. Yi, A. Acharya, R. Osborn, S. Rosenkranz, O. Chmaissem, and R. J. Birgeneau, *Phys. Rev. B* **98**, 180505(R) (2018).
 - [14] J. Ma, M. Yi, G. Affeldt, I. Hayes, C. Jozwiak, A. Bostwick, E. Rotenberg, J. Analytis, R. Birgeneau, and A. Lanzara, *Phys. Rev. B* **101**, 094515 (2020).
 - [15] M. Yi, Z.-X. Shen, and D. Lu, *npj Quant. Mater.* **2**, 57 (2017).

- [16] T.-M. Chuang, M. P. Allan, J. Lee, Y. Xie, N. Ni, S. L. Bud'ko, G. S. Boebinger, P. C. Canfield, and J. C. Davis, *Science* **327**, 181 (2010).
- [17] M. Yi, D. Lu, J.-H. Chu, J. G. Analytis, A. P. Sorini, A. F. Kemper, B. Moritz, S.-K. Mo, R. G. Moore, M. Hashimoto, W.-S. Lee, Z. Hussain, T. P. Devereaux, I. R. Fisher, and Z.-X. Shen, *Proc. Nat. Acad. Sci.* **108**, 6878 (2011).
- [18] W. T. Jin, Y. Xiao, Z. Bukowski, Y. Su, S. Nandi, A. P. Sazonov, M. Meven, O. Zaharko, S. Demirdis, K. Nemkovski, K. Schmalzl, L. M. Tran, Z. Guguchia, E. Feng, Z. Fu, and T. Brückel, *Phys. Rev. B* **94**, 184513 (2016).
- [19] J. Rodriguez-Carvajal, *Physica B* **192**, 55 (1993).
- [20] M. Zając, T. Giela, K. Freindl, J. Korecki, E. Madej, M. Sikora, N. Spiridis, M. Stankiewicz, J. Stępień, J. Szade, M. Ślęzak, T. Ślęzak, and D. Wilgocka-Ślęzak, *Synchr. Rad. Nat. Sci.* **19**, 1 (2020).
- [21] Y. K. Kim, W. S. Jung, G. R. Han, K.-Y. Choi, C.-C. Chen, T. P. Devereaux, A. Chainani, J. Miyawaki, Y. Takata, Y. Tanaka, M. Oura, S. Shin, A. P. Singh, H. G. Lee, J.-Y. Kim, and C. Kim, *Phys. Rev. Lett.* **111**, 217001 (2013).
- [22] C. Liu, T. Kondo, R. M. Fernandes, A. D. Palczewski, E. D. Mun, N. Ni, A. N. Thaler, A. Bostwick, E. Rotenberg, J. Schmalian, S. L. Bud'ko, P. C. Canfield, and A. Kaminski, *Nat Phys* **6**, 419 (2010).
- [23] P. Richard, K. Nakayama, T. Sato, M. Neupane, Y.-M. Xu, J. H. Bowen, G. F. Chen, J. L. Luo, N. L. Wang, X. Dai, Z. Fang, H. Ding, and T. Takahashi, *Phys. Rev. Lett.* **104**, 137001 (2010).
- [24] T. Morinari, E. Kaneshita, and T. Tohyama, *Phys. Rev. Lett.* **105**, 037203 (2010).
- [25] M. Matusiak, Z. Bukowski, and J. Karpinski, *Phys. Rev. B* **83**, 224505 (2011).
- [26] E. C. Blomberg, M. A. Tanatar, R. M. Fernandes, I. I. Mazin, B. Shen, H.-H. Wen, M. D. Johannes, J. Schmalian, and R. Prozorov, *Nat Commun* **4**, 1914 (2013).
- [27] B. Valenzuela, E. Bascones, and M. J. Calderón, *Phys. Rev. Lett.* **105**, 207202 (2010).
- [28] F. Bondino, E. Magnano, M. Malvestuto, F. Parmigiani, M. A. McGuire, A. S. Sefat, B. C. Sales, R. Jin, D. Mandrus, E. W. Plummer, D. J. Singh, and N. Mannella, *Phys. Rev. Lett.* **101**, 267001 (2008).
- [29] E. Z. Kurmaev, J. A. McLeod, A. Buling, N. A. Skorikov, A. Moewes, M. Neumann, M. A. Korotin, Y. A. Izyumov, N. Ni, and P. C. Canfield, *Phys. Rev. B* **80**, 054508 (2009).
- [30] W. L. Yang, A. P. Sorini, C.-C. Chen, B. Moritz, W.-S. Lee, F. Vernay, P. Olalde-Velasco, J. D. Denlinger, B. Delley, J.-H. Chu, J. G. Analytis, I. R. Fisher, Z. A. Ren, J. Yang, W. Lu, Z. X. Zhao, J. van den Brink, Z. Hussain, Z.-X. Shen, and T. P. Devereaux, *Phys. Rev. B* **80**, 014508 (2009).
- [31] M. Merz, F. Eilers, T. Wolf, P. Nagel, H. v. Löhneysen, and S. Schuppler, *Phys. Rev. B* **86**, 104503 (2012).
- [32] M. Merz, P. Schweiss, P. Nagel, M.-J. Huang, R. Eder, T. Wolf, H. von Löhneysen, and S. Schuppler, *J. Phys. Soc. Jap.* **85**, 044707 (2016).
- [33] J. Pellicciari, K. Ishii, M. Dantz, X. Lu, D. E. McNally, V. N. Strocov, L. Xing, X. Wang, C. Jin, H. S. Jeevan, P. Gegenwart, and T. Schmitt, *Phys. Rev. B* **95**, 115152 (2017).
- [34] J. J. Ying, X. F. Wang, T. Wu, Z. J. Xiang, R. H. Liu, Y. J. Yan, A. F. Wang, M. Zhang, G. J. Ye, P. Cheng, J. P. Hu, and X. H. Chen, *Phys. Rev. Lett.* **107**, 067001 (2011).
- [35] S. Jiang, H. S. Jeevan, J. Dong, and P. Gegenwart, *Phys. Rev. Lett.* **110**, 067001 (2013).
- [36] C.-C. Chen, J. Maciejko, A. P. Sorini, B. Moritz, R. R. P. Singh, and T. P. Devereaux, *Phys. Rev. B* **82**, 100504(R) (2010).
- [37] See Supplemental Material at <http://link.aps.org/supplemental/10.1103/PhysRevB.102.195126> for more information on the analysis of the XLD signal.
- [38] O. Bunău and Y. Joly, *J. Phys.: Cond. Matter* **21**, 345501 (2009).
- [39] G. van der Laan, E. Arenholz, R. V. Chopdekar, and Y. Suzuki, *Phys. Rev. B* **77**, 064407 (2008).
- [40] F. Nolting, D. Legut, J. Ruzs, P. M. Oppeneer, G. Woltersdorf, and C. H. Back, *Phys. Rev. B* **82**, 184415 (2010).
- [41] L. Ortenzi, H. Gretarsson, S. Kasahara, Y. Matsuda, T. Shibauchi, K. D. Finkelstein, W. Wu, S. R. Julian, Y.-J. Kim, I. I. Mazin, and L. Boeri, *Phys. Rev. Lett.* **114**, 047001 (2015).
- [42] Y. Kim, H. Oh, C. Kim, D. Song, W. Jung, B. Kim, H. J. Choi, C. Kim, B. Lee, S. Khim, H. Kim, K. Kim, J. Hong, and Y. Kwon, *Phys. Rev. B* **83**, 064509 (2011).
- [43] C.-C. Chen, B. Moritz, J. van den Brink, T. P. Devereaux, and R. R. P. Singh, *Phys. Rev. B* **80**, 180418(R) (2009).
- [44] A. Błachowski, K. Ruebenbauer, J. Żukrowski, Z. Bukowski, K. Rogacki, P. J. W. Moll, and J. Karpinski, *Phys. Rev. B* **84**, 174503 (2011).
- [45] S. Ikeda, K. Yoshida, and H. Kobayashi, *J. Phys. Soc. Jpn.* **81**, 033703 (2012).
- [46] F. Weber, D. Parshall, L. Pintschovius, J.-P. Castellan, M. Kauth, M. Merz, T. Wolf, M. Schütt, J. Schmalian, R. M. Fernandes, and D. Reznik, *Phys. Rev. B* **98**, 014516 (2018).
- [47] J. Li, P. J. Pereira, J. Yuan, Y.-Y. Lv, M.-P. Jiang, D. Lu, Z.-Q. Lin, Y.-J. Liu, J.-F. Wang, L. Li, X. Ke, G. V. Tendeloo, M.-Y. Li, H.-L. Feng, T. Hatano, H.-B. Wang, P.-H. Wu, K. Yamaura, E. Takayama-Muromachi, J. Vanacken, L. F. Chibotaru, and V. V. Moshchalkov, *Nat Commun* **8**, 1880 (2017).
- [48] A. Pal, M. Chinotti, J.-H. Chu, H.-H. Kuo, I. R. Fisher, and L. Degiorgi, *npj Quant Mater* **4**, 3 (2019).
- [49] P. J. Hirschfeld, *C. R. Phys.* **17**, 197 (2016).
- [50] T. Saito, S. Onari, and H. Kontani, *Phys. Rev. B* **82**, 144510 (2010).
- [51] P. Richard, T. Qian, and H. Ding, *J. Phys.: Cond. Mat.* **27**, 293203 (2015).